Photochemistry and Photobiology, 20**, **: *–*

A Bioscreening Technique for Ultraviolet Irradiation Protective Natural Substances

Jenni Tienaho[1,2]*, Emmi Poikulainen[1], Tytti Sarjala[2], Riina Muilu-Mäkelä[2], Ville Santala[1] and Matti Karp[1]

[1]Laboratory of Chemistry and Bioengineering, Tampere University of Technology, Tampere, Finland
[2]Natural Resources Institute Finland (Luke), Production systems, Parkano, Finland

Received 20 March 2018, accepted 28 May 2018, DOI: 10.1111/php.12954

ABSTRACT

Ultraviolet radiation (UV-R) causes genotoxic and aging effects on skin, and sunscreens are used to alleviate the damage. However, sunscreens contain synthetic shielding agents that can cause harmful effects in the environment. Nature-derived substances may have potential as replacement materials for the harmful sunscreen chemicals. However, screening of a broad range of samples is tedious, and often requires a separate genotoxicity assessment. We describe a simple microplate technique for the screening of UV protective substances using a recombinant *Escherichia coli* biosensor. Both absorbance-based and bioactivity-based shields can be detected with simultaneous information about the sample genotoxicity. With this technique, a controversial sunscreen compound, oxybenzone offers physical or absorbance-based shield but appears genotoxic at higher concentrations (3.3 mg/mL). We also demonstrate that pine needle extract (Pi_{Ne}) shields the biosensor from UV-R in a dose-dependent manner without showing genotoxicity. The physical shield of 5 mg/mL Pi_{Ne} was similar to that of one of the most common UV-shielding compound TiO_2 concentration 0.80 mg/mL. The bioactivity-based shield of Pi_{Ne} also reaches the extent of the physical shield with the highest concentration (3.3 mg/mL). We conclude that our technique is suitable in detecting the UV-shielding potential of natural substances, and gives simultaneous information on genotoxicity.

INTRODUCTION

Ultraviolet radiation (UV-R) is the main environmental cause of photo-induced skin aging by the process of producing free radicals, such as reactive oxygen species (ROS) in the skin cells. ROS stimulate inflammatory process, initiate DNA damage and cause oxidative damage to cellular lipids, proteins and carbohydrates (1). UV-R can also cause skin cancer by inducing carcinogenic effects. To alleviate these adverse consequences, sunscreen use is widely encouraged. Based on their mechanism of action, most sunscreen compounds used today can be separated into "physical sunscreens" or minerals, and "chemical sunscreens." Physical shielding compounds, such as titanium dioxide (TiO_2) and zinc oxide (ZnO), reflect, scatter and absorb UV-R. Chemical sunscreen compounds, such as oxybenzone, octinoxate, avobenzone or *para*-amino benzoic acid (PABA), contain alternating single and double bonds in their structure, which allows them to absorb the high-energy UV-R and release UV-R with lower energy (2). This process makes the radiation less damaging.

Both of these shielding compound groups have been found to have disadvantages. Physical sunscreens can cause a bleaching effect, which is unsightly but can be reduced by decreasing the particle size of the mineral used (3). However, the use of non-degradable and accumulating nanoparticles is causing emerging concern among the environmental scientists (4). Chemical UV filters also possess harmful environmental impacts. For example, (2-hydroxy-4-methoxyphenyl)-phenylmethanone (oxybenzone) has been shown to be genotoxic to coral planulae (5). Sunscreen components have also been demonstrated to induce coral bleaching by promoting viral infections to hard coral and their symbiotic algae (6). There is therefore an urgent need to replace sunscreen chemicals with more environmentally friendly options. This could be achieved using nature-derived substances with UV inhibition or shielding properties. The screening of vast amount of substances is, however, tedious and often requires a separate evaluation of the genotoxicity.

For the simultaneous assessment of genotoxicity, living whole-cell microbial biosensors have been proven to be useful. Living whole-cell microbial biosensors can detect both bioactivity and bioavailability of a selected sample material simultaneously, and the produced real-time response can be quantified and monitored in a continuous manner. For example, the *Escherichia coli* (*E. coli*) strain DPD2794 (7) has been constructed by fusing the SOS-responsive *recA* gene promoter of the bacteria with the luminescent *luxCDABE* genes of marine *Vibrio fischeri* bacteria. The resulting *recA'::lux* reporter plasmid produces an increase in the luminescent light emission in the presence of bioavailable genotoxic DNA damaging agents.

Sassanfar *et al.* (8) concluded that UV-R induces about 10-fold transcription of *recA*. This was later confirmed by Vollmer *et al.* (7) using the *E. coli* DPD2794 biosensor. They also found that the sensor was extremely sensitive and effective when compared to the conventional methodologies, such as the Ames test. Here, we have applied the biosensor to develop a microplate technique with high-throughput screening (HTS) potential, which can be easily used with any laboratory equipment emitting continuous UV-R, such as a standard polymerase chain reaction (PCR) cabinet. PCR cabinets are designed for nucleic acid amplification and UV-R is used to prevent sample contamination.

*Corresponding author emails: jenni.tienaho@tut.fi; jenni.tienaho@luke.fi (Jenni Tienaho)

Synthesis of UV-absorbing compounds in epidermal layers of plant leaves is one of the several mechanisms in plants to protect themselves against UV radiation. Needles of conifer species are known to be well protected from UV radiation (9,10). For example, Scots pine needles have been reported to accumulate UV-B inducible flavonoids for shielding the inner cell layers (11). Scots pine needles also comprise a vast resource of renewable side stream biomass in forestry to be utilized for novel purposes, and therefore, were selected as a suitable testing material for the method development.

Some nature-derived UV filters are already in use. The mechanism by which many of these work is based on secondary metabolites acting as antioxidant or anti-inflammatory agents, thereby alleviating the harmful effects of UV radiation (12). One commercially used example of a nature-derived chemical sunscreen compound is PABA, which can be found in yeast, bacteria and plants. However, its use has been banned in many countries as it can cause allergic reactions and irritation (13). This highlights the need for simultaneous genotoxicity assessment.

Current testing models for sunscreen products can be divided into *in vivo* and *in vitro* models, from which only *in vivo* testing involving irradiation of human subjects have been validated and is currently in use for the official solar protection factor (SPF) testing (14). In addition to spectrophotometric *in vitro* methods, approaches with simultaneous information on sample genotoxicity have also been developed with human cell cultivations (15). However, the use of bacterial biosensor cells increases the HTS potential of the developed technique for a wide range of sample material with regard to time- and cost efficiency.

In this study, we introduce a microplate technique with improved HTS potential for the UV-shield detection of various sample material using the *E. coli* DPD2794 biosensor. With the developed and optimized technique, both physical shielding and biological shielding—where the UV shielding effect of sample material is measured in contact with biosensor cells—can be detected and compared simply and rapidly, without any need for a separate genotoxicity assessment. We also demonstrate that the technique is suitable for the screening of natural product extracts in order to replace the harmful chemicals used in the sunscreen products with natural, sustainable and less damaging biochemical UV protectants.

MATERIALS AND METHODS

Chemicals and samples. Tryptone, yeast extract and agar were obtained from Labema, Finland; NaCl, KH_2PO_4 and dimethyl sulfoxide (DMSO) from Merck KGaA, Germany; Sodium salt of ampicillin, TiO_2 (<5 μm particle size and predominantly rutile), astaxanthin and $CaCl_2$ were from Sigma-Aldrich, USA; and K_2HPO_4 from VWR International, USA. M9 Minimal Salts mixture (containing Na_2HPO_4•7 H_2O, KH_2PO_4, NaCl and NH_4Cl) has been purchased from Sigma LifeSciences, Sigma-Aldrich, USA. $MgSO_4$ and L-ascorbic acid were obtained from J.T. Baker, USA, and D-glucose was from Amresco, USA. Ethanol was obtained from Altia, Finland and ciprofloxacin from Bayer, Germany. Finally, oxybenzone was obtained from TCI, Japan.

Bacterial strains and cultivation. Recombinant bacterial strain *E. coli* DPD2794 (*recA'::lux*) previously described by Vollmer *et al.* (7) was used in this study (a kind gift by Dr. Robert A. LaRossa from DuPont Company Central Research and Development, Wilmington, USA). The bacteria were preserved in 15% glycerol at −80°C. The working stock was prepared by inoculation in Lysogeny Agar (LA) (tryptone 10 g/L; yeast extract 5 g/L; NaCl 10 g/L and agar 15 g/L) growth-plates supplemented with 100 μg/mL of ampicillin and 100 mM of sterile and filtered potassium phosphate buffer, pH 7.0. The plates were cultivated overnight at 30°C before being stored at 4°C. A single colony of the strain was inoculated into 5 mL of liquid glucose-enriched M9 minimal medium (11.3 g/L M9 salts, 0.1 mM $CaCl_2$, 1 mM $MgSO_4$, and 0.2% (w/v) anhydrous D-Glucose) supplemented with 100 μg/mL of ampicillin. It was then incubated for approximately 16 h in a shaker at 30°C and 300 rpm, after which the luminescence was measured with a Chameleon Multilabel (Hidex Oy, Finland) microplate reader to verify the activity of the biosensor. Optical density at 600 nm was measured to be approximately 0.1 for the bacterial suspensions corresponding to 1×10^8 CFU/mL.

Sample preparation. The needle samples of Scots pine (*Pinus sylvestris* L.) were collected from a mature living pine from the western Finland during late June 2013. The needles of the previous of the current (c + 1) growing seasons were separated and weighed. Needles were frozen at −80°C and ground in a mortar with the help of liquid nitrogen before adding to sealed and previously weighed polypropylene test tubes. Pure methanol extraction was chosen because it has been reported to give high polyphenol content (16) and primary metabolites such as amino acids and sugars are not present in methanol extracts. For the extraction procedure, 27 mL of methanol (Methanol for liquid chromatography, LiChrosolv®, Merck KgaA, Germany) was mixed to 1.75 g of the needle powder by vortexing. Extraction tube was then put to the rotamixer (Rotamixer, Type MMVI4, Heto-Holten A/S, Denmark) at full power (30 rpm) for 60 min. Extraction tube was then centrifuged at +4°C and 8200 ***g*** for 10 min after which the supernatant was collected to a new polypropylene tube and finally filtered through nylon syringe filter (0.20 μm, Nylon 66 Filter Membrane from Supelco by Sigma-Aldrich Co, USA) to a previously weighed and sterile polypropylene test tube. Aliquot of methanol without needle material went through the same extraction procedure simultaneously as control sample. Finally, the extraction product was dried using a vacuum centrifuge with a cooling unit (Rotational-Vacuum-Concentrator RVC 2-18, Cold Trap CT 02-50 SR, Martin Christ Gefriertrocknungsanlagen GmbH, Germany) before storing at −80°C.

The dry and frozen methanol extract of pine needles was dissolved into methanol and double distilled water (DDW) (1:2.7) to achieve a stock solution of 100 mg/mL of dried extraction product. This stock solution was further diluted in DDW to achieve concentrations of 0.1; 0.5; 1.0 and 5.0 mg/mL for the physical shield testing and 0.17; 0.33; 1.7 and 3.3 mg/mL per microplate well for the biological shield tests. The difference in the concentrations chosen for the physical and biological shield tests is due to the stronger effect of the sample material when in direct contact with the bacterial biosensor cells. Hence, the sample concentrations for the biological test were kept slightly lower. The maximum concentration of the UV filters allowed in cosmetic products according to the EU Cosmetics Regulation list (Regulation (EC) 1223/2009) goes from 2% to 25% of the cosmetic product mass. We use a concentration maximum of 1% for the potential UV protective samples, which lays below these regulated maximum values. The highest methanol concentrations for the extracts were 1.4% for 5 mg/mL and 0.9% for 3.3 mg/mL. The sample solutions were stored in −20°C and covered from the light.

Irradiation source. DNA/RNA UV-cleaner cabinet (UVC/T-AR DNA/RNA UV-CLEANER BOX, BIOSAN company, Latvia) was used as the irradiation source for the experiments. This equipment was chosen because it is widely available in laboratories, and so requires no expensive investments. However, the developed technique can be adapted to any other continuous UV-R emitting setting and is therefore highly modifiable. The distance between the bottom of the microplate and the UV source was 48.5 cm for all of the measurements. The wavelength of the UV irradiation was validated using AvaSpec—ULS2048L StarLine Versatile Fiber-optic Spectrometer (Avantes, Apeldoorn, Netherlands), and it was that of a normal mercury UV lamp with a maximum wavelength of approximately 254 nm. Irradiation dose of the used cabinet was also measured using Ophir Laser thermal sensor 3A-PF-12 detector (Ophir Optronics Solutions Ltd, Jerusalem, Israel) with a 12 mm aperture.

Biological protection and bioactivity. With this technique, the sample volume of 50 μL of the potential UV protective substance concentrations was pipetted in triplicates into an opaque white 96-well microplate (Greiner Bio-one GmbH, Austria). The volume of 100 μL of the bacterial inoculation in M9 minimal media was then pipetted into the same microplate wells. For the sake of comparability, a clear UV-transparent microplate (Corning® 96 well plates, half-area, polystyrene flat bottom, UV-Vis-transparent between 220 and 1600 nm, Corning Inc.,

USA) containing 100 μL of water was added above the plate before irradiation. To stabilize the UV-R dose, the lamp, acting as a UV source, was left on for approximately 30 min before irradiation. The plates were then moved to a DNA/RNA UV-cleaner cabinet into a previously optimized place, and irradiated for 30 s with direct UV light. Some wells of the plate covered with aluminum foil sheet, for the negative control signals. After the irradiation period, 100 μL of Lysogeny Broth (LB) medium was added into the wells for nutrition and the luminescent light signal was measured in counts per second (CPS) using a Chameleon Multilabel (Hidex Oy, Finland) microplate reader in 10-minute intervals for a total of 180 min with a shaking between the measurements.

Physical protection and absorbance. This technique was otherwise similar to that of biological protection except that 100 μL of the different concentrations of the potential UV protective substances were pipetted in triplicates into clear UV transparent microplates in a way that the total liquid volume of the microplate wells remained the same. The 100 μL of bacterial inoculation in M9 minimal media was then added similarly into another separate opaque white microplate and the plates were then handled and irradiated as above.

Absorbance measurements. The absorbance of 100 μL of sample substance triplicates in translucent microplate (Sarstedt AG & Co, Germany) was evaluated using Thermo Scientific Varioskan Flash Reader (Thermo Fischer Scientific, Thermo Electron Co. USA) in the absorbance scan mode with 5 nm intervals for the wavelength area of 200–900 nm. Absorbance value averages were calculated and error bars are the standard deviations of the sample triplicates.

Result analysis. All figures have been drawn using Origin 8 data analysis and graphic workspace (OriginLab Corp., USA). Because CPS values can vary depending on the date and chosen culture, all of the results, except for the absorbance measurements, are expressed in induction factors (IF), which have been calculated by dividing the sample triplicate CPS value averages with those of negative controls. Error bars have been calculated from the standard deviations of the sample IF triplicates. A two-tailed *t*-test was also conducted to confirm the statistical significance of the results within the measurement plates using Microsoft Office Excel 2016 (Microsoft Co., USA).

RESULTS AND DISCUSSION

The wavelength of the UV irradiation was that of normal mercury lamp with a maximum in the 254 nm UV wavelength area and the irradiation dose rate was found to be approximately 190 $\mu W\ cm^{-2}$. The place of the microplate was optimized in the UV-cleaner cabinet to give the highest signal to background ratio and lowest errors between sample triplicates. The place was obtained when the plate was situated at 20 cm from the opening and 26 cm from the left face of the cabinet (see Fig. 1A). It was also found that the best irradiation time giving the maximum signal was 30 s and this time was used for the measurements throughout (Fig. 1B), making the irradiation dose 5.7 $mJ\ cm^{-2}$. The Standard Erythema Dose (SED) has been proposed by Commission Internationale de l'Eclairage (17) as UV-R dose equivalent of 100 $J\ m^{-2}$ or 10 $mJ\ cm^{-2}$ (18), and the used irradiation dose in this study is 57% of this. The incubation time is the time after exposure at which the luminescence signals were monitored every 10 min for 180 min, whereas the exposure time is the seconds of UV-R exposure. We can see that 30 s of irradiation gives the highest signal in the higher measurement times, and therefore, it has been chosen for the measurements. From Fig. 1C, we can see how the UV transparent clear microplate is put directly on top of the white opaque microplate with biosensor cells for the time of the UV exposure. The sample is placed into the clear plate above, for the physical measurements, and into the white microplate below, for the biological shield measurements.

We also tested to see whether the distance from the lamp height of the plate would affect the signal. We used a standard adjustable laboratory equipment jack (Lab Jack Swiss Boy 110 MR, Rudolf Grauer AG, Degersheim, Switzerland) for this. We found that the height of the plate was approximately directly proportional to the signal (See Figure S1). However, the normal table height was chosen for the measurements because it was the easiest to maintain, and the luminescent light signal produced was not efficiently lower than that of the highest setting.

TiO_2 (<5 μm particle size and predominantly rutile) was chosen to act as a known UV-shield control because it is extensively used in sunscreen products worldwide. However, TiO_2 is insoluble in water, and was dissolved into 96% ethanol to prepare 1 M solution and further diluted with DDW for concentrations of 0.80; 8.0; 80 and 800 μg/mL. The ethanol percentages of the final solutions were 0.00032–3.2%. TiO_2 has been shown to possess antimicrobial effects (19) and also the uneven distribution of small insoluble particles could affect the microbial cell functions. Therefore, among cells the control used was LB growth medium because it absorbs the UV-R wavelengths. The LB was diluted with DDW to get dry matter concentrations of 0.01; 0.09; 0.93 and 9.3 mg/mL per microplate well. The results obtained from these standard substances are shown in Fig. 2A (TiO_2) and 2B (LB) from where we can see that they provide UV protection in a dose-dependent manner with all of the LB concentrations except the lowest of 0.01 mg/mL of dry matter concentration and with the highest 800 and 80 μg/mL of TiO_2.

To verify the effectiveness of the UV-R dose used, we also compared the induced signals of UV-R to that induced with a known antibiotic ciprofloxacin (50 mg/mL stock solution was diluted to DDW to achieve concentrations of 0.001; 1.0; 3.8; 5.5 and 7.5 mg/mL per microplate well). Ciprofloxacin specifically targets the bacterial DNA and the obtained results can be seen in Fig. 3A. From the figure, we can see that the exposure time of 30 s gives approximately the same luminescence light signal induction factor at the time point of 100 min after exposure time with the ciprofloxacin concentration of 0.001 mg/mL. With higher concentrations of ciprofloxacin, it seems that the light signal produced starts to decrease, which is probably due to cell death, and therefore reduction in the sum of the luminescent light signal produced by the bacteria in the microplate well. These results show that the UV-R dose chosen is effective enough to be comparable with the genotoxic effects toward the bacteria caused by a known antibiotic.

It is also widely known that antioxidants can prevent the damage induced by UV-R by targeting the induced production of ROS in the cell. The known antioxidants L-ascorbic acid (0.17; 0.33; 0.83; 1.7 and 3.3 mg/mL per microplate well in DDW) and astaxanthin (5 mg/mL solution was prepared in DMSO, and DDW was used to achieve concentrations of 0.017; 0.17; 1.7; 17 and 170 μg/mL per microplate well) were used to test this protection mechanism in the developed methodologies. From Fig. 3B, it can be seen that ascorbic acid seems to give biological shield against UV light in a dose-dependent manner and Fig. 3C shows that ascorbic acid concentrations also absorb the UV wavelengths under 300 nm. However, the shielding effect is not as clear in the case of astaxanthin (Fig. 3D). Astaxanthin also seems to induce the luminescence production with all but the lowest concentrations (0.017 and 0.17 μg/mL per microplate well) implying genotoxic properties. However, as astaxanthin stock was dissolved into DMSO, the solvent used most likely causes this observation. The astaxanthin concentrations used were from 1.7×10^{-5} to 0.17 mg/mL, and they consequently contain from 0.0003 to 3.3% DMSO, and this could produce

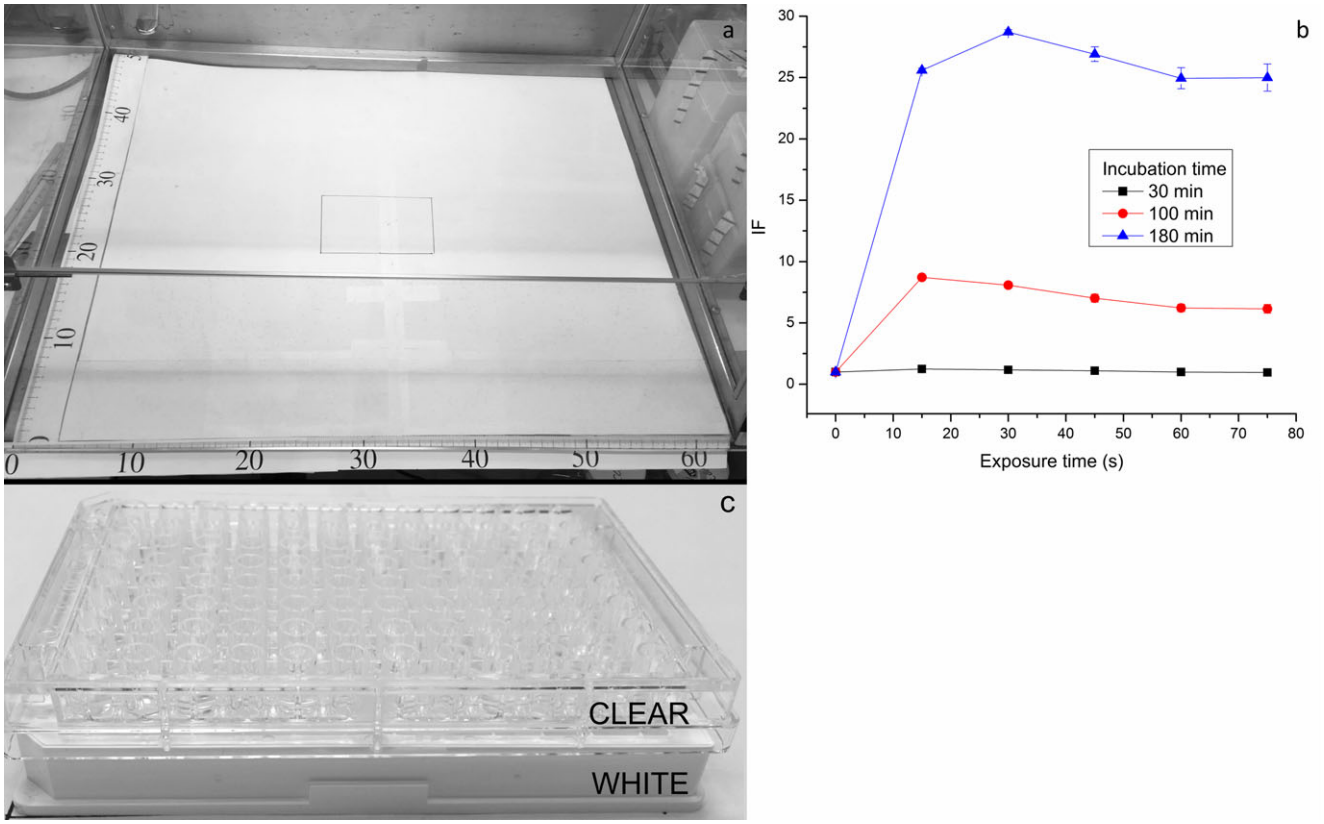

Figure 1. The optimal place of the microplate in the UV-cleaner cabinet for obtaining the highest signal to background ratio and smallest errors between triplicate measurements (a). The exposure time signals at 30, 100 and 180 min of incubation after exposure to UV-R (b). Clear UV transparent microplate placed directly over the opaque white microplate with the biosensor bacteria. In physical shield measurements, the sample is put on a clear plate, and in biological shield measurements on a white plate (c).

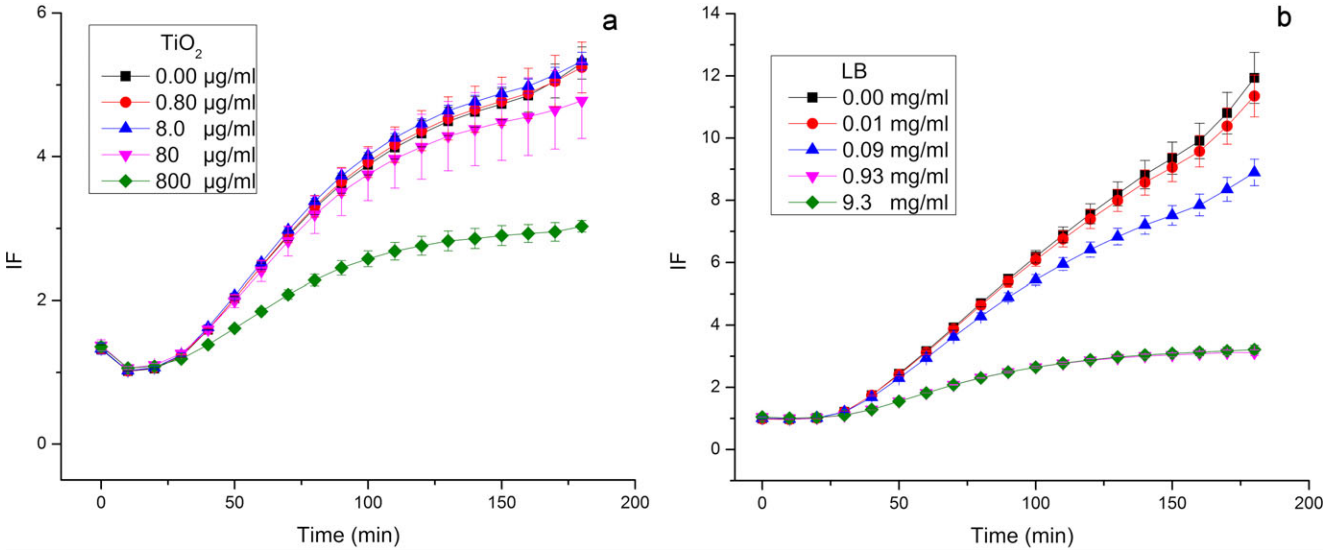

Figure 2. Luminescence produced by the *E. coli* DPD2794 biosensor, when exposed to 30 s of UV light while protected by (a) TiO_2 concentrations with physical protection measurement (in a separate UV plate) and (b) LB concentrations with biological protection (in contact with bacterial cells) measurement.

enough toxicity in the higher concentrations. In fact, due to this result, we tested that the biosensor can stand no larger concentrations than 2% of DMSO without it affecting the cells (data not shown). DMSO has also previously been found to possess bacteriostatic properties (20). From the absorbance of these substances, we can see that DMSO itself absorbs in the UV area (Fig. 3E) but in the biological shield technique (Fig. 3D), the shielding effect is lost due to genotoxicity. The sample with the

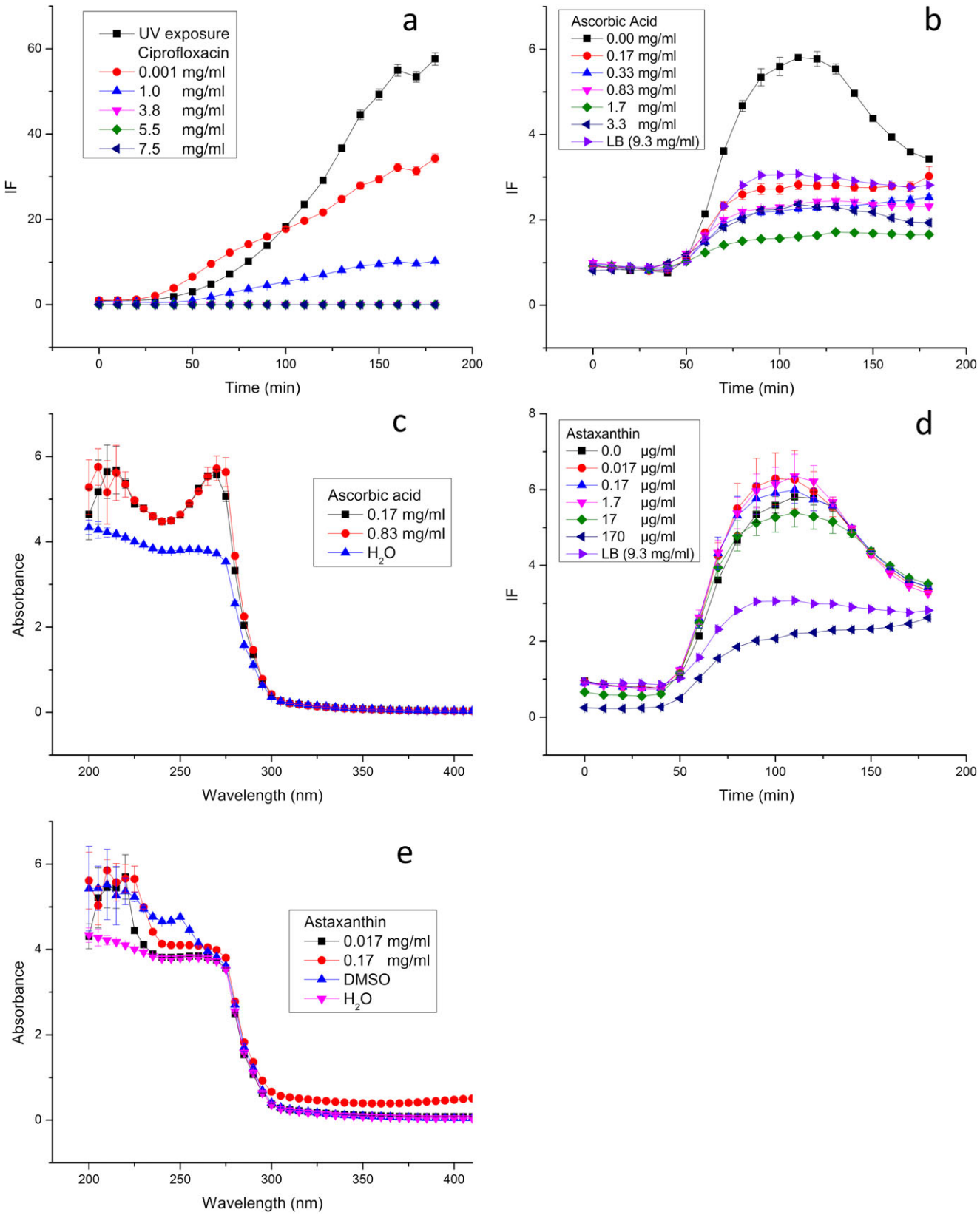

Figure 3. The comparison of the effect of the UV-R dose of 30 s to that of ciprofloxacin concentrations (a). The luminescence signals produced by *E. coli* DPD2794 when exposed to 30 s of UV radiation while protected by antioxidant agent ascorbic acid (b) and astaxanthin (d) concentrations as well as LB controls. All substances have been measured with contact with the bacterial cells (biological effect). The absorbance of the ascorbic acid (c) and astaxanthin (e) and the corresponding controls in the different wavelength areas.

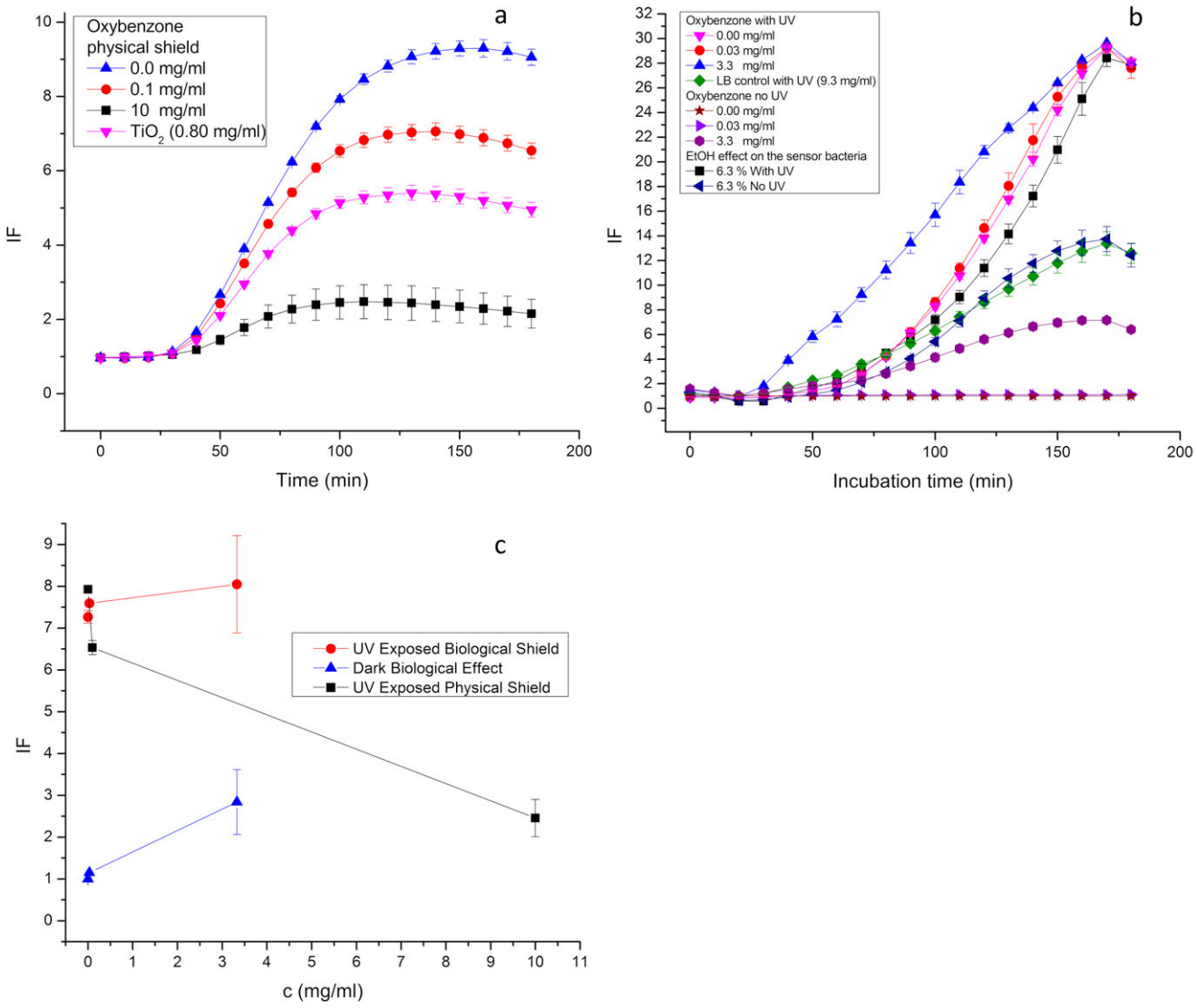

Figure 4. UV shielding effects and genotoxicity of oxybenzone. Physical (a) and biological (b) shielding and their comparison at the time point 100 min (c). In addition to other figures, the dark biological effect was added in which the cells have not been UV-irradiated.

highest concentration of astaxanthin (170 µg/mL) at 100 min of the measurement gave better shield for the biosensor than the LB control, as the IF of the astaxanthin sample was smaller than the unprotected cells (0 µg/mL) and the LB control (P values < 0.0001). According to the results, also the sample with 3.3 mg/mL ascorbic acid shields the biosensor from the UV-R better than the LB control. The lower IF of the ascorbic acid sample than that of LB or non-shielded biosensor cells (P values < 0.0001) indicates statistically significant shielding. This observation of antioxidants causing UV shielding effects is not surprising as UV-R causes ROS formation. Astaxanthin has been referred as the most effective antioxidant but unfortunately the insolubility to water causes it to be not as preferable source of shield according to our technique. By adding antioxidant material into sunscreens, the risks caused by UV-R can, however, be alleviated.

Because oxybenzone has been found to be harmful toward coral planulae and its effect was found to be increased by the exposure to UV light (5), we were curious on finding out, how it would affect our genotoxicity sensitive biosensor. The oxybenzone stock of 50 mg/mL was prepared by dissolving oxybenzone into 96% ethanol. Further dilutions of 10 and 0.1 mg/mL were prepared into DDW for the physical shield testing, whereas concentrations of 0.03 and 3.3 mg/mL per microplate well were used for the biological activity test (consequently they contained 0.63–6.3% of ethanol). As expected, we found that oxybenzone possesses physical UV-shield (Fig. 4A), whereas biological shielding effect (Fig. 4B) is overtaken by the genotoxicity of the chemical and the ethanol concentrations do not explain these observations, when biosensor cells are exposed to both oxybenzone and UV-R. In Fig. 4C, the physical and biological shield from Fig. 4A,B of the sample are drawn at the time point 100 min. From Fig. 4C, we can see that the physical shield shows dose-dependent behavior, but as the bacterial cells are already harmed by the oxybenzone itself (dark biological effect shows dose-dependent rise in luminescence signal levels), adding UV exposure significantly increases the luminescent light signal production indicating severe DNA damage instead of shielding

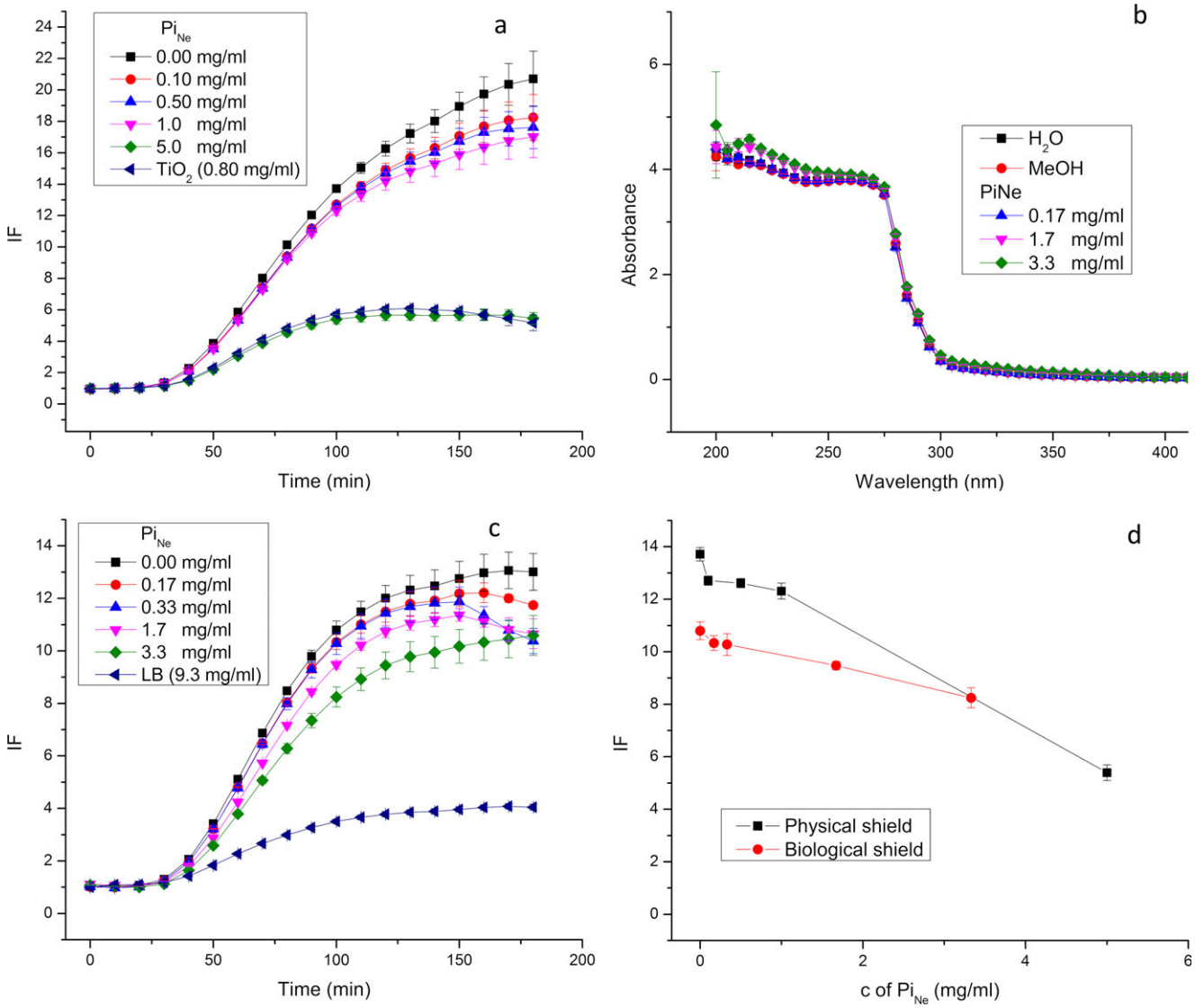

Figure 5. Luminescent light signal produced when *E. coli* DPD2794 cells were exposed to 30 s of UV radiation and protected by pine needle methanol extract concentrations (Pi_{Ne}). The physical shield results (a), the absorbance of the sample in the different wavelength areas (b), the biological shield results (c) and the comparison of the methods (d) are shown with the used sample concentrations.

effect. At 100 min of the measurement, the UV exposed oxybenzone (3.3 mg/mL) caused more DNA damage to the biosensor cells than the unexposed oxybenzone with same concentration, as its signal is higher than that of the unexposed (P value < 0.0001). This 3.3 mg/mL oxybenzone concentration at 100 min measurement time also caused more damage to the biosensor cells than the mere UV exposure (P value = 0.002). This information indicates that these results represent statistical significance. The results underline that, while oxybenzone has physical UV-shielding effect, it is also harmful to the biosensor cells and similar adverse results have been previously reported in the case of coral and fish (5,6,21). Oxybenzone has also been shown to cause contact or photocontact allergy or even urticarial reactions with humans (21).

A potential source to obtain safe and sustainable UV-shielding compounds is nature-derived substances. The methodology was tested using *Pinus sylvestris* L. needle extract (Pi_{Ne}) and the results are shown in Fig. 5. Pine needles are exposed to the UV-R from the sun and therefore, they are expected to possess UV inhibitory activity, which we were able to demonstrate with our technique. Figure 5A,B corresponds to the physical absorbance based shield, and we can see that they absorb in the UV area. The Pi_{Ne} with concentration 5.0 mg/mL protects the biosensor cells from adverse effects of the UV-R, as its IF in 100 min measurement is lower than that of the unprotected sample (P value < 0.0001). In addition, this protective capacity is similar to that of a commercially used sunscreen chemical TiO_2 concentration 0.80 mg/mL, which was used as a control (P value = 0.1683, tested for difference in means). Methanol extractable polyphenols are known for their antioxidant activities, which can correspond to the biological shielding potential shown in Fig. 5C. The highest concentration of Pi_{Ne} (3.3 mg/mL) exhibits biological UV-R protective properties for the biosensor cells. This is demonstrated in the 100 min measurement results, where the IF for the Pi_{Ne} is lower than that for the unprotected cells (P value = 0.001). However, the IF of the Pi_{Ne} is higher than that

of the LB control (P value < 0.0001), which indicates that it is not as effective in the protection as the LB control. In Fig. 5D, the comparison of the effectiveness of the physical and biological shielding mechanisms shows that the absorbance based (physical) shield is the main factor corresponding to the UV inhibition of the used extract concentrations, whereas we cannot detect any genotoxicity. Nature-derived substances are therefore potentially less harmful to the environment and they also pose no similar risk of accumulation to the environment as mineral-based physical sunscreen nanoparticles because they are degradable and, as in this case of needles, sustainably derived from a waste-stream of forestry. Although the biological shielding in our technique was not as high as with control substance LB, the methanol extracts are most likely rich in polyphenols and flavonoids, which have been widely reported to have antioxidant properties (16). These results should, however, be considered to be merely indicative of the applicability of the technique developed. For a more comprehensive analysis of the UV protection capacity of the selected needle material, test should be performed with a broad range of needle material samples gathered from various environments and at different times of year.

In conclusion, it is important to obtain safe, sustainable and environmentally friendly UV-shielding compounds. Our methodology can be utilized and is also highly modifiable to be used in the high-throughput screening of various natural products for UV-R induced damage preventive substances and it gives simultaneous information about the genotoxic effects of the sample substance.

CONFLICT OF INTEREST

The authors declare that they have no conflicts of interest.

Acknowledgements—The European Regional Development Fund has supported this work (project code A71142). The town of Parkano and SASKY municipal education and training consortium also contributed to funding this work, along with Natural Resources Institute Finland and Tampere University of Technology. We wish to thank Dr. Matti Virkki for the help with the wavelength and UV dose measurements and analyses as well as Dr. Praveen Ramasamy, who kindly offered us the astaxanthin powder. Dr. Robert A. LaRossa from DuPont Company Central Research and Development, kindly provided the *E. coli* DPD2794 bacterial strain.

SUPPORTING INFORMATION

Additional supporting information may be found online in the Supporting Information section at the end of the article:

Figure S1. The effect of the plate distance from the irradiation source.

REFERENCES

1. Pillai, S., C. Oresajo and J. Hayward (2005) Ultraviolet radiation and skin aging: roles of reactive oxygen species, inflammation and protease activation, and strategies for prevention of inflammation induced matrix degradation – a review. *Int. J. Cosmet. Sci.* **27**, 17–34.
2. Heinrich, U., H. Tronnier, D. Kockott, R. Kuckuk and H. M. Heise (2004) Comparison of sun protection factors determined by an *in vivo* and different *in vitro* methodologies: a study with 58 different commercially available sunscreen products. *Int. J. Cosmet. Sci.* **26**, 79–89.
3. Kockler, J., M. Oelgemöller, S. Robertson and B. D. Glass (2014) Influence of titanium dioxide particle size on the photostability of the chemical UV-filters butyl methoxy dibenzoylmethane and octocrylene in a microemulsion. *Cosmetics* **1**, 128–139.
4. Lu, J., S. Tian, X. Lv, Z. Chen, B. Chen, X. Zhu and Z. Cai (2018) TiO_2 nanoparticles in the marine environment: impact on the toxicity of phenanthrene and Cd^{2+} to marine zooplankton *Artemia salina*. *Sci. Total Environ.* **615**, 375–380.
5. Downs, C., E. Kramarsky-Winter, R. Segal, J. Fauth, S. Knutson, O. Bronstein, F. Ciner, R. Jeger, Y. Lichtenfeld, C. Woodley, P. Pennington, K. Cadenas, A. Kushmaro and Y. Lova (2016) Toxicopathological effects of the sunscreen UV filter, oxybenzone (Benzophenone-3), on coral planulae and cultured primary cells and its environmental contamination in Hawaii and the U.S. Virgin Islands. *Arch. Environ. Contam. Toxicol.* **70**, 265–288.
6. Danovaro, R., L. Bongiorni, C. Corinaldesi, D. Giovannelli, E. Damiani, P. Astolfi, L. Greci and A. Pusceddu (2008) Sunscreens cause coral bleaching by promoting viral infections. *Environ. Health Perspect.* **116**, 441–447.
7. Vollmer, A. C., S. Belkin, D. R. Smulski, T. K. Van Dyk and R. A. LaRossa (1997) Detection of DNA damage by use of *Escherichia coli* carrying recA':lux, uvrA':lux, or alkA':lux reporter plasmids. *Appl. Environ. Microbiol.* **63**, 2566–2571.
8. Sassanfar, M. and J. Roberts (1991) Constitutive and UV-mediated activation of RecA protein: combined effects of recA441 and recF143 mutations and of addition of nucleosides and adenine. *J. Bacteriol.* **173**, 5869–5875.
9. Day, T. A., T. C. Vogelmann and E. H. DeLucia (1992) Are some plant life forms more effective than others in screening out ultraviolet-B radiation? *Oecologia* **92**, 513–519.
10. Hoque, E. and G. Remus (1999) Natural UV-screening mechanisms of Norway spruce (*Picea abies* [L.] Karst.) needles. *Photochem. Photobiol.* **69**, 177–192.
11. Schnitzler, J.-P., T. P. Jungblut, C. Feicht, M. Köfferlein, C. Langebartels, W. Heller and H. Sandermann (1997) UV-B induction of flavonoid biosynthesis in Scots pine (*Pinus sylvestris* L.) seedlings. *Trees* **11**, 162–168.
12. Saewan, N. and A. Jimtaisong (2015) Natural products as photoprotection. *J. Cosmet. Dermatol.* **14**, 47–63.
13. Wong, T. and D. Orton (2011) Sunscreen allergy and its investigation. *Clin. Dermatol.* **29**, 306–310.
14. Cole, C. (2014) Sunscreens – what is the ideal testing model? *Photodermatol. Photoimmunol. Photomed.* **30**, 81–87.
15. Schuch, A. P., M. C. S. Moraes, T. Yagura and C. F. M. Menck (2014) Highly sensitive biological assay for determining the photoprotective efficacy of sunscreen. *Environ. Sci. Technol.* **48**, 11584–11590.
16. Sowndhararajan, K. and S. C. Kang (2012) Free radical scavenging activity from different extracts of leaves of Bauhinia vahlii Wight & Arn. *Saudi J. Biol. Sci.* **20**, 319–325.
17. Commission Internationale de l'Eclairage (1997) *Standard Erythema Dose, A Review. Technical Report CIE 125-1997*. CIE Central Bureau, Vienna, Austria.
18. IARC Working Group on the Evaluation of Carcinogenic Risk to Humans (2012) Solar and Ultraviolet Radiation. In *Radiation - IARC Monographs on the Evaluation of Carcinogenic Risks to Humans*, No. 100D. pp. 35–102. International Agency for Research on Cancer, Lyon, France.
19. Besinis, A. T., De Peralta and R. D. Handy (2014) The antibacterial effects of silver, titanium dioxide and silica dioxide nanoparticles compared to the dental disinfectant chlorhexidine on *Streptococcus mutans* using a suite of bioassays. *Nanotoxicology* **8**, 1–16.
20. Wood, D. C. and J. Wood (1975) Pharmacologic and biochemical considerations of dimethyl sulfoxide. *Ann. N. Y. Acad. Sci.* **243**, 7–19.
21. DiNardo, J. and C. A. Downs (2017) Dermatological and environmental toxicological impact of the sunscreen ingredient oxybenzone/benzophenone-3. *J. Cosmet. Dermatol.* **17**, 15–19.